Journal of Biomolecular NMR, 9 (1997) 306–312
ESCOM

J-Bio NMR 449

Stereospecific assignment of the NH_2 resonances from the primary amides of asparagine and glutamine side chains in isotopically labeled proteins

Lawrence P. McIntosh[a,*], Emmanuel Brun[a] and Lewis E. Kay[b,*]

[a]*Protein Engineering Network Centers of Excellence, Department of Biochemistry and Molecular Biology and Department of Chemistry, University of British Columbia, Vancouver, BC, Canada V6T 1Z3*
[b]*Protein Engineering Network Centers of Excellence and Departments of Medical Genetics, Biochemistry and Chemistry, University of Toronto, Toronto, ON, Canada M5S 1A8*

Received 7 March 1997
Accepted 24 March 1997

Keywords: Primary amide; Stereospecific assignment; HMQC spectroscopy; Dihedral angle

Summary

An HMQC-based pulse scheme is presented for the stereospecific assignment of asparagine and glutamine side-chain amide protons. The approach makes use of the recently developed quantitative-J correlation spectroscopy [Bax, A. et al. (1994) *Methods Enzymol.*, **239**, 79–105] to distinguish the *E* and *Z* primary amide protons and, as such, eliminates the need for assignments derived from more time-consuming and potentially ambiguous NOE methods. An application of this method to a uniformly ^{15}N,^{13}C-labeled cellulose-binding domain is presented. When used in combination with a NOESY-HSQC experiment, the predominant χ_2 dihedral angles of two asparagine side chains in this protein can also be defined.

Asparagine and glutamine residues play important structural roles in proteins, protein–DNA and protein–carbohydrate complexes, due to the ability of their primary amide groups to act as both hydrogen bond acceptors and donors. Accordingly, the complete assignment of the resonances of these side chains is necessary for characterizing accurately the structures and functions of proteins by NMR spectroscopy. Although several methods have been developed for the selective detection of NH_2 signals (Kay and Bax, 1989; Farmer and Venters, 1996), in practice, these resonances are readily identified in the conventional ^1H-^{15}N HSQC spectrum of a uniformly ^{15}N-labeled protein as a pair of peaks sharing a common nitrogen shift near 112 ppm (Wishart et al., 1995). Furthermore, in the presence of ~10% D_2O lock solvent, a set of distinct 'shadow' peaks, displaced upfield in the nitrogen dimension by a one-bond deuterium isotope shift of ~–0.5 ppm, is typically observed due to exchange yielding ^{15}NHD groups. Traditionally, the primary amide proton resonances of asparagines and glutamines were assigned to specific residues within a protein using intraside-chain NOE correlations (Wüthrich, 1986). With the advent of triple-resonance ^1H-^{13}C-^{15}N NMR spectroscopy, these assignments can now be obtained unambiguously using scalar correlations observed through a variety of approaches, including the HNCO, HNCACB, CBCA(CO)NH, C(CO)-NH, and H(CCO)NH experiments (Grzesiek and Bax, 1992; Montelione et al., 1992; Grzesiek et al., 1993; Wittekind and Mueller, 1993; Farmer and Venters, 1996; Johnson et al., 1996).

Due to hindered rotation about the C-N partial double bond, the geminal protons of primary amides interconvert slowly on the NMR timescale and thus are detected with distinct chemical shifts (Redfield and Waelder, 1979).

*To whom correspondence should be addressed.

The nomenclature for the side chains of asparagine and glutamine, illustrated in Fig. 3, follows that recommended by the IUPAC-IUBMB-IUPAB Interunion Task Group. The commonly used names of *cis* and *trans* refer to the orientation of the nitrogen-bonded proton relative to the carbonyl oxygen, with the *trans* proton (*E*; $H^{\delta 21}$ or $H^{\varepsilon 21}$) lying *anti* or opposite to the oxygen and the *cis* proton (*Z*; $H^{\delta 22}$ or $H^{\varepsilon 22}$) lying *syn* or adjacent to the oxygen.

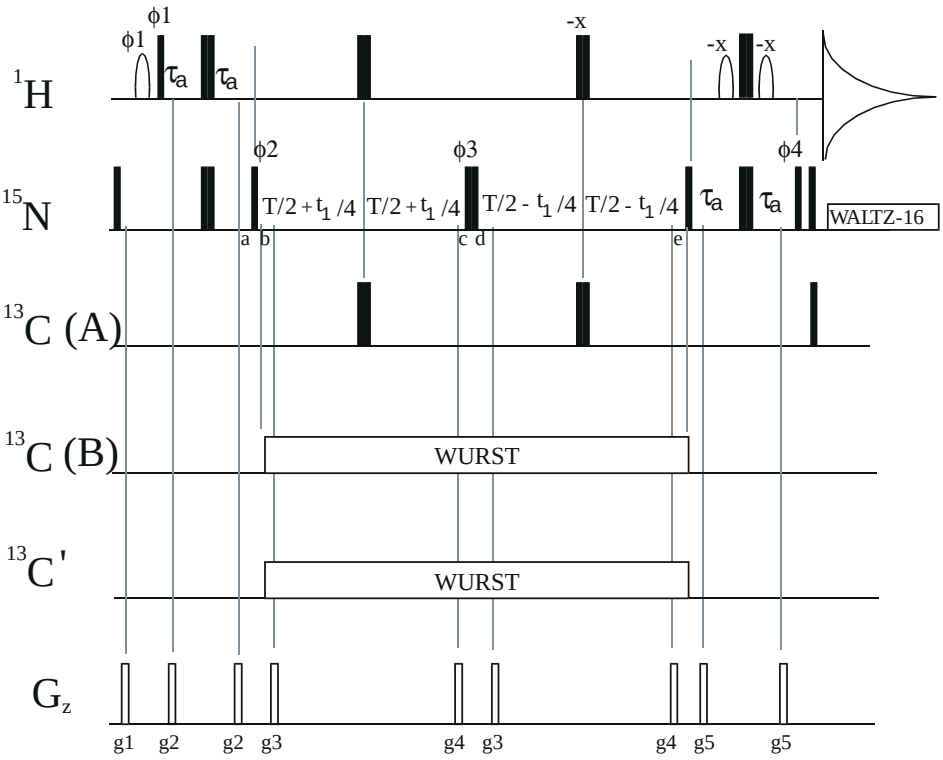

Fig. 1. Pulse sequences for the stereospecific assignment of asparagine and glutamine primary amide NH_2 protons. In scheme A, ^{13}C (A) is included and ^{13}C (B) is omitted, whereas in scheme B, the reverse applies. All narrow (wide) rectangular pulses have a flip angle of 90° (180°). ^{1}H, ^{13}C and ^{15}N pulses are centered at 4.7 ppm (water), 35 ppm and 119 ppm, respectively. The field strengths used for rectangular pulses are 24 kHz (^{1}H), 5.4 kHz (^{15}N) and 19.6 kHz (^{13}C). The composite proton 180° pulses applied during the 2T period are of the form $90_y\,180_x\,90_y$ (Freeman et al., 1980). ^{15}N decoupling during acquisition is achieved using a 1.4 kHz WALTZ-16 field (Shaka et al., 1983). Decoupling is preceded by a $90_{\phi4}\,90_x$ ^{15}N pair (Bax et al., 1990) and by a ^{13}C 90° pulse (see text). The first water-selective 90° pulse (phase ϕ1) has the E-Burp-1 profile (Geen and Freeman, 1991) and a duration of 8 ms. The final pair of water-selective 90° pulses have a duration of 2.0 ms and are rectangular in shape (Piotto et al., 1992). The phase of each of the water-selective pulses is adjusted to minimize the residual water signal. Carbonyl decoupling is achieved with a WURST-2 decoupling scheme (Kupce and Freeman, 1995) centered at 176 ppm, with a band width of ±830 Hz (500 MHz spectrometer frequency). Each WURST pulse has a duration of 3 ms, a maximum rf amplitude of 530 Hz and is divided into 5000 steps. Decoupling fields are generated using a five-step supercycle (0° 60° 150° 60° 0°; Tycko et al., 1985) of the WURST pulses. Aliphatic carbon decoupling (scheme B; ^{13}C (A) is omitted and ^{13}C (B) is included) employs a WURST-2 scheme centered at 42 ppm with a band width of ±2.6 kHz and a maximum rf amplitude of 0.94 kHz. Each of the WURST pulses is 3 ms and divided into 5000 steps as before. In the case of scheme B, the aliphatic and carbonyl decoupling sequences are added to generate a single waveform. Both the carbonyl and carbonyl/aliphatic decoupling waveforms were constructed using the Pbox toolkit provided in the Varian software. The delays τ_a and T are set to 2.4 ms and between 12 and 35 ms, respectively. The phase cycle employed is: ϕ1 = (x,–x); ϕ2 = (x); ϕ3 = 2(x),2(y),2(–x),2(–y); ϕ4 = 8(x),8(–x); acq = (x,–x,–x,x). Quadrature detection in F1 is achieved by States-TPPI (Marion et al., 1989) phase cycling of ϕ2. The strengths and durations of the gradients are: g1 = (1 ms, 8 G/cm); g2 = (0.5 ms, 30 G/cm); g3 = (0.2 ms, 7.5 G/cm); g4 = (0.1 ms, 25 G/cm); g5 = (0.12 ms, 15 G/cm). Decoupling is interrupted prior to the application of the gradients (Kay, 1993). All spectra were recorded on a Varian UNITY 500 MHz spectrometer equipped with a triple-resonance probe and pulsed field gradient capabilities.

This presents an avenue to increase the accuracy by which the conformations of asparagine or glutamine side chains can be defined in NMR-derived structures of proteins, provided that the amide proton resonances are assigned stereospecifically. In random coil polypeptides, the *Z* ($H^{\delta22}$ or $H^{\varepsilon22}$) protons of asparagine or glutamine have chemical shifts of approximately 6.9 ppm, whereas those of the *E* ($H^{\delta21}$ or $H^{\varepsilon21}$) protons fall near 7.5 ppm (Wishart et al., 1995). Of course, within the context of a folded protein, this chemical shift pattern may be reversed due to factors such as hydrogen bonding or close proximity to aromatic rings. Therefore, the stereospecific assignments of the amide resonances from each asparagine and glutamine side chain must be determined experimentally. In a limited number of cases to date, these assignments have been deduced from the relative intensities of intraresidue NOEs to side-chain aliphatic protons (Anet and Bourn, 1965; Redfield and Waelder, 1979; Montelione et al., 1984). However, an approach based upon scalar correlations is desirable to avoid possible ambiguities associated with NOE methods including χ_2 or χ_3 dihedral angle-dependent aliphatic–amide interproton distances (see below), chemical shift degeneracies and spin diffusion. It is interesting to note that, in model amide compounds, the $^1J_{N\text{-}H}$ coupling between ^{15}N and the *Z* proton is 90.2 ± 0.9 Hz, whereas the coupling with the *E* proton is 93.2 ± 1.3

Hz (Bystrov, 1976). This suggests the possibility of deriving the stereospecific assignments of primary amide protons from accurate measurements of one-bond ^{15}N-^{1}H scalar couplings (Tolman and Prestegard, 1996). In the present communication, we present an alternative approach based on the recently developed method of quantitative-J correlation spectroscopy (Bax et al., 1994).

In a pioneering study of the ^{13}C NMR spectra of simple amides, Dorman and Bovey (1973) reported a $^{3}J_{C\text{-}H}$ coupling of 7.1 Hz between the methyl carbon of acetamide (CH_3CONH_2) and its amide *Z* proton (i.e. *syn* to the carbonyl oxygen and *anti* to the methyl) and negligible coupling to the *E* proton. This three-bond C-C'-N-H coupling was assigned due to its absence in *N*-methylacetamide, which adopts exclusively a *trans* conformation with the *N*-methyl group *syn* to the carbonyl oxygen. As emphasized by Bystrov (1976), the presence of this coupling can be exploited to stereospecifically assign the nitrogen-bonded protons in primary amides. Here we report a 2D ^{1}H-^{15}N HMQC-based experiment for the stereospecific assignment of NH_2 protons in asparagine and glutamine side chains of uniformly $^{13}C/^{15}N$-enriched proteins. Stereospecific assignments of the primary amide protons are derived immediately by inspection of the data presented in the form of a difference spectrum (see below). After completion of this study, we noted that Löhr and Rüterjans (1997) also used these $^{3}J_{C\text{-}H}$ couplings to discriminate side-chain NH_2 protons based on cross-peak splitting patterns in an H_2NCO-E.COSY spectrum.

Figure 1 illustrates the quantitative-J correlation pulse schemes employed for the stereospecific assignment of primary amide NH_2 protons. The approach makes use of a 2D difference experiment. In the first scheme, A (i.e. the pulses on the line in Fig. 1 labeled as ^{13}C (A) are included while those on the line labeled ^{13}C (B) are not), side-chain NH magnetization is allowed to evolve with respect to the three-bond coupling to the $^{13}C^{\beta}$ (Asn) or $^{13}C^{\gamma}$ (Gln) nucleus, whereas in the second sequence, B, evolution due to this coupling is suppressed. Magnetization originating on the side-chain $H^{\delta 2*}$ (Asn) or $H^{\varepsilon 2*}$ (Gln) evolves due to ^{1}H-^{15}N scalar coupling for a period of $2\tau_a$ and is largely antiphase with respect to the attached nitrogen spin at point a in the sequence. Subsequent application of the 90° ^{15}N pulse of phase $\phi 2$ establishes double and zero quantum coherence, which is allowed to evolve for a constant-time period of duration 2T. During this time, ^{15}N chemi-

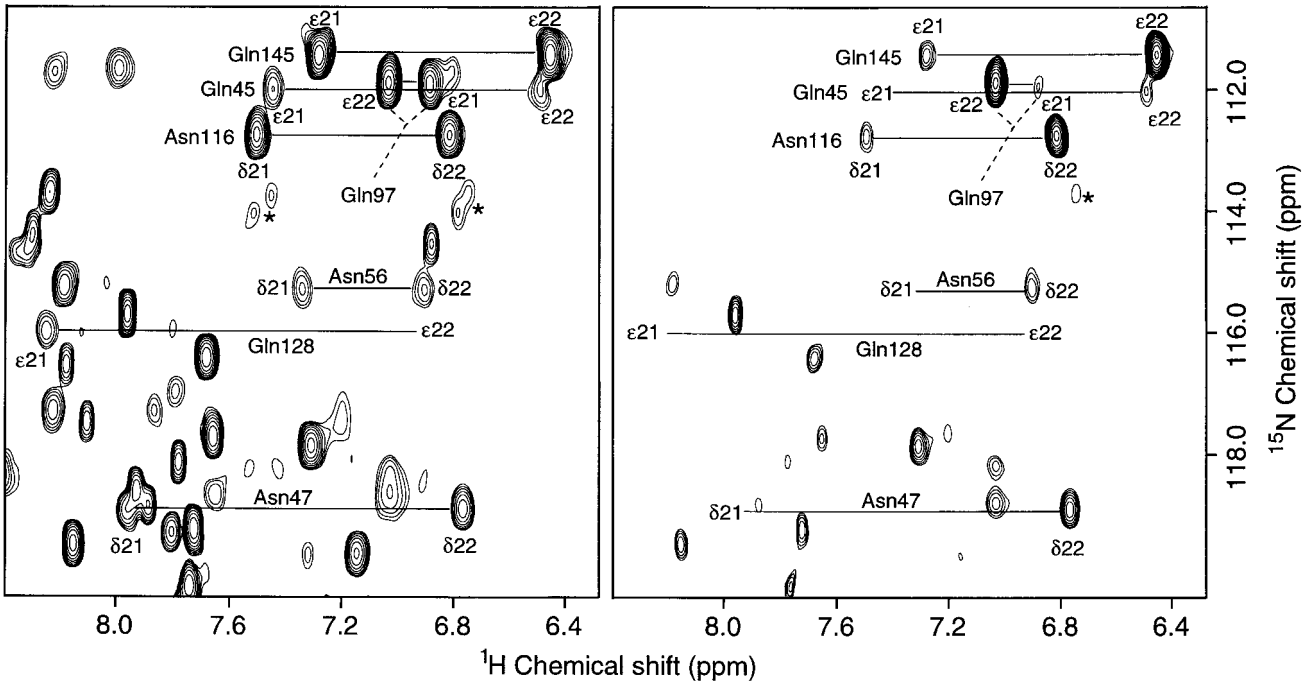

Fig. 2. The primary amide region of the EZ-HMQC-NH_2 spectrum of uniformly $^{15}N/^{13}C$-labeled CBD_{N2} recorded with scheme B (left) and the difference spectrum (B – A; right), displayed at the same contour level. The pairs of ^{1}H-^{15}N peaks arising from each of the three asparagine and four glutamine residues are connected by horizontal lines. In the difference spectrum, the peaks from the *Z* ($H^{\delta 22}$ or $H^{\varepsilon 22}$) protons appear with significantly greater intensities than those from the corresponding *E* ($H^{\delta 21}$ or $H^{\varepsilon 21}$) protons, leading to the indicated stereospecific assignments. In the case of Gln^{128}, the $H^{\varepsilon 21}$ is present in the spectrum recorded with scheme B and missing in the difference spectrum, whereas the $H^{\varepsilon 22}$ is very weak in both spectra and thus not observed at this contour level. Additional peaks in the spectra arise from the main-chain secondary amides. A pair of weak NH_2 peaks due to degraded or modified forms of CBD_{N2} in the year-old sample are indicated with an asterisk (*). The spectra were recorded on a ~0.8 mM sample of protein (50 mM NaCl, 50 mM potassium phosphate, 0.02% NaN_3, pH 6.0, 10% D_2O/90% H_2O, 35 °C) in the presence of saturating quantities of cellopentaose. Data from sequences A and B were recorded in an interleaved fashion using T = 22 ms (^{1}H: 640 complex points collected with SW = 6500 Hz; ^{15}N: 69 complex points collected with SW = 1600 Hz) and processed with FELIX 2.05 (Biosym-MSI Inc., San Diego, CA, U.S.A.). The total acquisition time was 3.5 h.

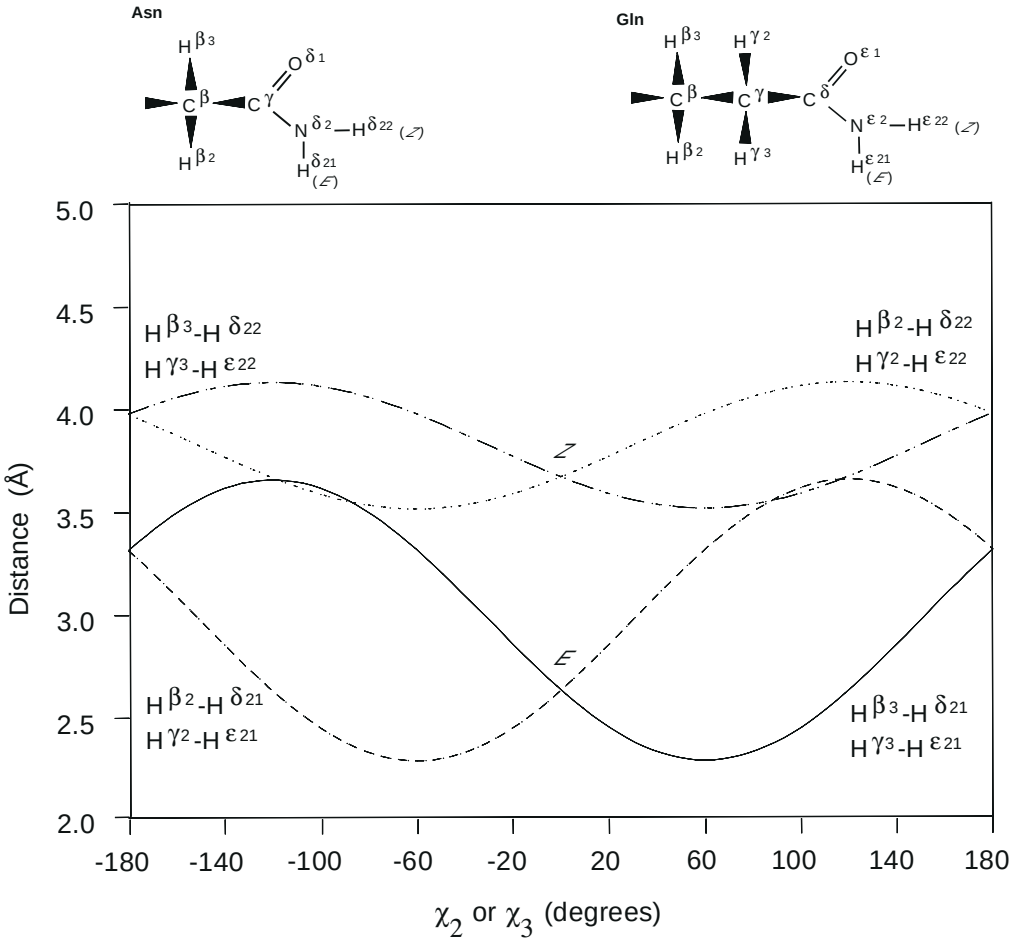

Fig. 3. Dependence of the intraresidue proton–proton distances between the $H^{\beta 2}/H^{\beta 3}$ (or $H^{\gamma 2}/H^{\gamma 3}$) and $H^{\delta 21}/H^{\delta 22}$ (or $H^{\varepsilon 21}/H^{\varepsilon 22}$) protons in asparagine (or glutamine) residues on the χ_2 (or χ_3) dihedral angle. The *E* ($H^{\delta 21}$ or $H^{\varepsilon 21}$) proton is always closer to a methylene side-chain proton than is the *Z* ($H^{\delta 22}$ or $H^{\varepsilon 22}$) proton, thus allowing stereospecific assignments of the primary amide protons to be obtained based upon relative NOE intensities. If the methylene H^{β} or H^{γ} protons are also stereospecifically assigned, it is possible to define the χ_2 or χ_3 dihedral angle of the asparagine or glutamine side chain, respectively. The figure was generated using the atomic coordinates of asparagine defined in the X-PLOR 3.1 topology and parameter files. The nomenclature used throughout this communication for the side chains of asparagine and glutamine is illustrated. Dihedral angles are defined such that 0° corresponds to a conformation with C^{α} (or C^{β}) and the side-chain carbonyl oxygen eclipsed.

cal shift is recorded and evolution due to ^1H chemical shift is refocussed by the composite ^1H 180° pulses applied between points b and c and points d and e. The simultaneous application of ^1H and ^{13}C 180° pulses in scheme A ensures that the three-bond $^{13}C^{\beta}$-$H^{\delta 2*}$ or $^{13}C^{\gamma}$-$H^{\varepsilon 2*}$ scalar coupling ($J_{C\text{-}H}$) evolves for the complete constant-time duration, 2T, and attenuates the signal by a factor of $\cos(2\pi J_{C\text{-}H} T)$. In contrast, evolution does not occur in sequence B, as ^{13}C aliphatic decoupling is applied throughout the complete 2T period. At the conclusion of the constant-time period, the double and zero quantum coherences are converted into ^1H magnetization, which is then refocussed during the subsequent $2\tau_a$ period prior to detection. An (optional) ^{15}N $90_{\phi 4}90_x$ pulse pair is applied immediately prior to acquisition, as discussed previously by Bax et al. (1990). In the case of sequence A, where ^1H-^{13}C scalar coupling is allowed to evolve during the 2T period, the antiphase proton signal that builds up due to $J_{C\text{-}H}$ during this period is eliminated by the action of the ^{13}C 90° pulse immediately before acquisition. Because the signal originates on the labile NH_2 protons in these experiments, it is critical to minimize saturation/dephasing of water magnetization (Grzesiek and Bax, 1993; Kay et al., 1994; Stonehouse et al., 1994). This is accomplished using the 'water' selective pulses applied during the course of experiments A and B. Data from schemes A and B are recorded in an interleaved manner and stored in separate memory locations. The ratio of cross-peak intensities, S, obtained from each of the experiments is given by $S_A/S_B = \cos(2\pi J_{C\text{-}H} T)$, allowing quantitative measurement of $J_{C\text{-}H}$. Additionally, in a difference spectrum (B – A), the amide *Z* protons, which have the largest couplings to the side-chain ^{13}C nuclei and thus exhibit the greatest changes in cross-peak intensities, can be readily identified by inspection. With this in mind, the present experiment is referred to as EZ-HMQC-NH_2.

EZ-HMQC-NH_2 spectra of a uniformly $^{13}C/^{15}N$-enriched CBD_{N2} complexed with cellopentaose are presented in Fig. 2. CBD_{N2} is the second of the tandem N-terminal cellulose-binding domains from *Cellulomonas fimi* endoglucanse C. The pairs of ^{1}H-^{15}N peaks from the primary amides of the three asparagine and four glutamine residues in this 153-residue (15.9 kDa) domain were assigned using a series of ^{1}H-^{13}C-^{15}N correlation experiments and will be reported elsewhere (see also Johnson et al., 1996). In the difference spectrum (B – A), the cross peak from the member of each pair arising from the *Z* ($H^{\delta 22}$ or $H^{\varepsilon 22}$) proton is significantly stronger than the peak from the corresponding *E* ($H^{\delta 21}$ or $H^{\varepsilon 21}$) partner, leading immediately to the indicated stereospecific assignments. In accordance with the 'random coil' chemical shifts of asparagine and glutamine, the *Z* protons of six of the seven primary amides in CBD_{N2} resonate upfield from their partner *E* protons. However, this pattern is reversed in the case of Gln^{97}, for which the chemical shift of the *Z* ($H^{\varepsilon 22}$) proton is *downfield* from that of the *E* ($H^{\varepsilon 21}$) proton. Based on a preliminary low-resolution structure of CBD_{N2}, the perturbed chemical shifts of Gln^{97} are attributed to a ring current effect due to the adjacent Tyr^{111}.

A simultaneous analysis of EZ-HMQC-NH_2 spectra of CBD_{N2} recorded with T = 12 and 27 ms gave average measured $^{3}J_{C\beta\text{-}H\delta 22}$ and $^{3}J_{C\gamma\text{-}H\varepsilon 22}$ coupling constants of 7.0 ± 0.5 Hz, with no obvious dependence upon amino acid type or side-chain environment. This value agrees closely with that observed for the *Z* proton of acetamide (Dorman and Bovey, 1973). However, in contrast to the negligible coupling between the methyl carbon and amide *E* proton reported for this model compound, a similar analysis of the spectra in Fig. 2 reveals that small $^{3}J_{C\beta\text{-}H\delta 21}$ or $^{3}J_{C\gamma\text{-}H\varepsilon 21}$ couplings of less than approximately 1.5 Hz exist for the primary amides of asparagine and glutamine.

The significant difference between the magnitudes of

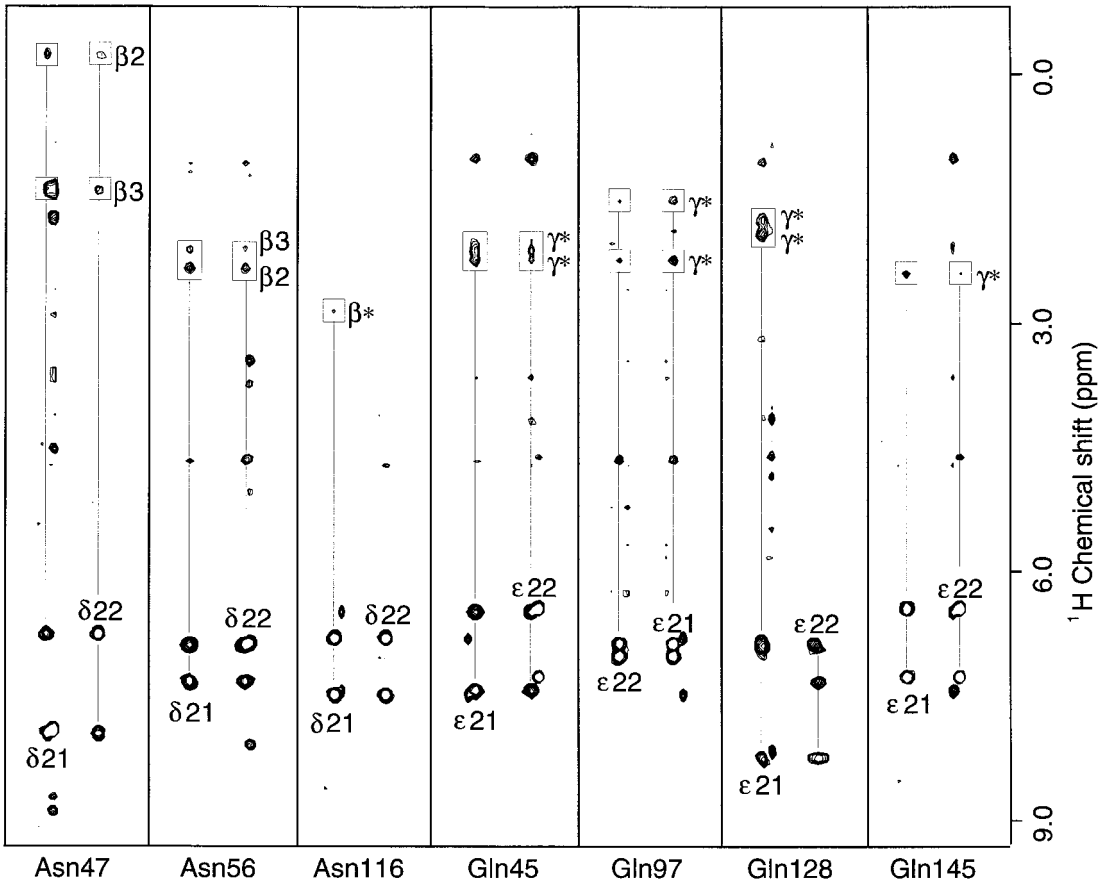

Fig. 4. ^{1}H-^{1}H strip plots from the 3D sensitivity-enhanced ^{15}N-resolved NOESY-HSQC spectrum (Zhang et al., 1994) of uniformly ^{15}N-labeled CBD_{N2} (τ_{mix} = 90 ms; total acquisition time ~3 days). The diagonal peaks from the primary amides of the asparagine and glutamine residues and the cross peaks arising from intraresidue NOEs with their side-chain methylene protons are labelled. The horizontal axis is arranged such that the strip corresponding to the amide proton from each NH_2 group with the more downfield chemical shift is to the left. Consistent with the stereospecific assignments derived from the EZ-HMQC-NH_2 experiment and the intraresidue amide–aliphatic proton–proton distances illustrated in Fig. 3, the relative intensities of the NOEs from the H^{β} or H^{γ} to the *E* ($H^{\delta 21}$ or $H^{\varepsilon 21}$) amide proton are greater than those to the *Z* ($H^{\delta 22}$ or $H^{\varepsilon 22}$) proton. The $H^{\beta 2}$ and $H^{\beta 3}$ of Asn^{47} and Asn^{56} were assigned stereospecifically based upon the analysis of short-mixing-time TOCSY-HSQC (Zhang et al., 1994) and HNHB experiments (Archer et al., 1991), according to a staggered rotomer model. Non-stereospecifically assigned prochiral protons are indicated by an asterisk (*).

the three-bond $^3J_{C\text{-}H}$ couplings to the *Z* and *E* protons, combined with their relative uniformity, indicates that a qualitative analysis of the EZ-HMQC-NH_2 experiment is sufficient to provide stereospecific assignments for the primary amides of asparagine and glutamine side chains, irrespective of their structural context within a polypeptide or protein. Inspection of the spectra in Fig. 2 does, however, reveal considerable variation in the intensities of the signals from each amide, reflecting different relaxation and exchange properties. In the cases of Gln^{97}, Asn^{116}, and Gln^{145}, which have intense NH_2 signals, large peaks from the *Z* ($H^{\delta 22}$ or $H^{\varepsilon 22}$) and small peaks from the *E* ($H^{\delta 21}$ or $H^{\varepsilon 21}$) protons are observed in the difference spectrum. In contrast, Gln^{45} and Asn^{56} exhibit weaker NH_2 signals, and thus the peaks from the *Z*, but not the *E* protons are observed in the difference spectrum at the chosen contour level. Finally, only the $^1H^{\delta 21}$ signal from Gln^{128} is detected in the spectrum recorded with scheme B (a weak $^1H^{\delta 22}$-^{15}N cross peak is observed in a gradient-enhanced HSQC spectrum of the protein; data not shown). The stereospecific assignment of the Gln^{128} *E* proton was deduced by its clear absence in the difference spectrum. In principle, for $2\pi J_{C\text{-}H} T \ll 1$, intensities of cross peaks in the difference spectrum are maximized by setting T to $T_2(N_xI_x)$, where $1/T_2(N_xI_x)$ is the average double/zero quantum relaxation rate of a side-chain ^{15}N-H spin pair. However, in practice, the reported stereospecific assignments of CBD_{N2} could be determined from spectra recorded with T values ranging from 12 to 32 ms (not shown).

In addition to the primary amides, strong peaks from tryptophan indole groups are observed in EZ-HMQC-NH_2 difference spectra of proteins due to two- and three-bond $H^{\varepsilon 1}/^{15}N^{\varepsilon 1}$-aromatic carbon couplings. Note that the aromatic carbons are not completely inverted by the ^{13}C 180° pulses in scheme A, nor are they properly decoupled using the WURST decoupling profile applied in B. Numerous weak peaks from main-chain NH groups also appear in the difference spectrum, reflecting a variety of possible intraresidue or sequential couplings between the H^N and ^{13}C nuclei within two or three bonds. The EZ-HMQC-NH_2 experiment should help to identify non-proline residues in *cis*-peptide bonds, for which a $^3J_{C\alpha_{(i-1)}\text{-}H^N{}_{(i)}}$ coupling of ~7 Hz is expected. However, the effects of homonuclear proton couplings such as $^3J_{H^N{}_{(i)}\text{-}H\alpha_{(i)}}$, which are active throughout much of the pulse scheme, significantly attenuate correlations involving backbone NH groups, and thus may complicate the identification of such main-chain amides.

Stereospecific assignments of the primary amide protons of asparagine and glutamine side chains have been obtained previously based upon the relative intensities of NOE cross peaks to the intraresidue H^β or H^γ, respectively. Figure 3 illustrates that, for all χ_2 or χ_3 dihedral angles, the *E* ($H^{\delta 21}$ or $H^{\varepsilon 21}$) proton is closer to at least one H^β or H^γ proton than is the *Z* proton. Therefore, the amide protons can be distinguished based upon the relative intensities of their NOEs with the adjacent methylene protons. ^1H-^1H planes from the 3D ^{15}N-resolved NOESY-HSQC spectrum of uniformly ^{15}N-labeled CBD_{N2} (Fig. 4) confirm that the stereospecific assignments obtained by this NOE method agree with those obtained using the EZ-HMQC-NH_2 experiment. Indeed, the two approaches are very complementary in that the former identifies the *E* proton by virtue of stronger intraresidue NOEs, while the latter identifies the *Z* proton based upon larger $^3J_{C\text{-}H}$ couplings. For example, in CBD_{N2} only the peak from the (*E*) $H^{\varepsilon 21}$ proton of Gln^{128} is observed in the EZ-HMQC-NH_2 spectrum recorded with scheme B of Fig. 1, leading to a stereospecific assignment deduced by its *absence* in the difference spectrum. However, this assignment is readily confirmed by the strong intraresidue NOE cross peaks between the $H^{\gamma *}$ and $H^{\varepsilon 21}$ of this glutamine in a ^{15}N-resolved NOESY-HSQC spectrum (Fig. 4).

A clear advantage of the EZ-HMQC-NH_2 experiment is that the stereospecific assignments are based upon uniform scalar couplings that, to the first approximation, are independent of the structure of the protein. The peaks from primary amides are generally well resolved in a ^1H-^{15}N correlation spectrum and, furthermore, identification of these *Z* and *E* protons can be made in the complete absence of any additional spectral assignments. The EZ-HMQC-NH_2 can be recorded in a few hours of spectrometer time. However, the experiment does require a uniformly $^{13}C/^{15}N$-labeled protein sample. In addition, T_2 relaxation will impose a size limitation on this method, although deuteration of the aliphatic carbons will help offset this effect to some degree. In contrast, the NOE-based approach can be applied to small, unlabeled proteins or ^{15}N-labeled proteins of intermediate size, and thus does not require a potentially expensive $^{13}C/^{15}N$ sample. However, obvious disadvantages of the latter approach include the longer acquisition times required for 2D or 3D NOESY spectra, the necessity for side-chain proton assignments, and potential problems due to spectral overlap (e.g. the $H^{\delta 21}$-$H^{\beta 3}$ NOE peak of Asn^{47} overlaps a nearby NOE peak from a main-chain amide; Fig. 4), weak or absent NOEs (e.g. Asn^{116} and Gln^{145}), dihedral angle-dependent aliphatic–amide interproton distances, conformational averaging about χ_2 or χ_3, and spin diffusion.

As is evident from Fig. 3, it is possible to use NOE information to define the χ_2 dihedral angle of an asparagine side chain, provided that the resonances from the amide $H^{\delta 21}/H^{\delta 22}$ and aliphatic $H^{\beta 2}/H^{\beta 3}$ nuclei are all stereospecifically assigned. Several approaches have been developed to assign the prochiral H^β of these side chains (Powers et al., 1993). This same argument holds for glutamine, although in general it is more difficult to obtain stereospecific assignments of the H^γ protons. As an example, in CBD_{N2} the pattern of NOE intensities of

$H^{\delta 21}$-$H^{\beta 3}$ > $H^{\delta 21}$-$H^{\beta 2}$ ~ $H^{\delta 22}$-$H^{\beta 3}$ > $H^{\delta 22}$-$H^{\beta 2}$ for Asn^{47} indicates that the χ_2 dihedral angle of this side chain is positive, falling near +120° (Figs. 3 and 4). In contrast, for Asn^{56}, χ_2 is near −120° based on the relative NOE intensities of $H^{\delta 21}$-$H^{\beta 2}$ > $H^{\delta 21}$-$H^{\beta 3}$ ~ $H^{\delta 22}$-$H^{\beta 2}$ > $H^{\delta 22}$-$H^{\beta 3}$. However, from a quantitative analysis of the NOE cross peaks, it is likely that some degree of rotomer averaging occurs for both of these side chains. As summarized by Ponder and Richards (1987), the χ_2 (or χ_3) dihedral angles for asparagine (or glutamine) residues in high-resolution crystal structures of proteins vary considerably and are not restricted to a few predominant rotomeric states. Therefore, caution must be exercised to avoid over-restraining the dihedral angles of these residues based upon a qualitative analysis of NOE intensity patterns. Nevertheless, it is important to stress that in X-ray crystallographic analyses of proteins, the O and NH_2 of the primary amides are in general not distinguishable. Thus, the orientations of the amide groups, and hence χ_2 (Asn) or χ_3 (Gln) dihedral angles, are usually set based upon consistent patterns of hydrogen-bonding interactions to neighboring atoms. In contrast, the ability of NMR methods to directly detect nitrogen-bonded protons provides an experimental approach for determining the conformation(s) of primary amides within the side chains of asparagine and glutamine residues in a protein.

In summary, we have described a simple and sensitive scheme for the stereospecific assignment of side-chain amide protons of asparagine and glutamine residues, based exclusively on scalar connectivities. In combination with the stereospecific assignments of either H^{β} (Asn) or H^{γ} (Gln) resonances and relative intensities of the NOEs connecting the amide and methylene protons, it is also possible to estimate the χ_2 and χ_3 dihedral angles for these residues.

Acknowledgements

This work was supported through grants from the Natural Sciences and Engineering Research Council of Canada (L.E.K.), the Medical Research Council of Canada (L.E.K.), and the Protein Engineering Network of Centers of Excellence (L.P.M. and L.E.K.). The authors thank Drs. R. Muhandiram (University of Toronto) for assistance with data analysis, P. Legault (University of Toronto) for a sample used to develop the pulse sequence methodology, Lisa Gentile (University of British Columbia) and Malcolm McArthur (University College London) for helpful comments, and E. Kupce (Varian) for assistance with using the Pbox toolkit for the construction of the decoupling profiles used in the experiments.

References

Anet, F.A.L. and Bourn, A.J.R. (1965) *J. Am. Chem. Soc.*, **87**, 5250–5251.

Archer, S.J., Ikura, M., Torchia, D.A. and Bax, A. (1991) *J. Magn. Reson.*, **95**, 636–641.

Bax, A., Clore, G.M. and Gronenborn, A.M. (1990) *J. Magn. Reson.*, **88**, 425–431.

Bax, A., Vuister, G.W., Grzesiek, S., Delaglio, F., Wang, A.C., Tschudin, R. and Zhu, G. (1994) *Methods Enzymol.*, **239**, 79–105.

Bystrov, V.F. (1976) *Prog. NMR Spectrosc.*, **10**, 41–81.

Dorman, D.E. and Bovey, F.A. (1973) *J. Org. Chem.*, **38**, 1719–1722.

Farmer II, B.T. and Venters, R.A. (1996) *J. Biomol. NMR*, **7**, 59–71.

Freeman, R., Kempsell, S.P. and Levitt, M.H. (1980) *J. Magn. Reson.*, **38**, 453–479.

Geen, H. and Freeman, R. (1991) *J. Magn. Reson.*, **93**, 93–141.

Grzesiek, S. and Bax, A. (1992) *J. Am. Chem. Soc.*, **114**, 6291–6293.

Grzesiek, S., Anglister, J. and Bax, A. (1993) *J. Magn. Reson.*, **B101**, 114–119.

Grzesiek, S. and Bax, A. (1993) *J. Am. Chem. Soc.*, **115**, 12593–12594.

Johnson, P.E., Joshi, M.D., Tomme, P., Kilburn, D.G. and McIntosh, L.P. (1996) *Biochemistry*, **35**, 14381–14394.

Kay, L.E. and Bax, A. (1989) *J. Magn. Reson.*, **84**, 598–603.

Kay, L.E. (1993) *J. Am. Chem. Soc.*, **115**, 2955–2057.

Kay, L.E., Xu, G.Y. and Yamazaki, T. (1994) *J. Magn. Reson.*, **A109**, 129–133.

Kupce, E. and Freeman, R. (1995) *J. Magn. Reson.*, **A115**, 273–276.

Löhr, F. and Rüterjans, H. (1997) *J. Magn. Reson.*, **124**, 255–258.

Marion, D., Ikura, M., Tschudin, R. and Bax, A. (1989) *J. Magn. Reson.*, **85**, 393–399.

Montelione, G.T., Arnold, E., Meinwald, Y.C., Stimson, E.R., Denton, J.B., Huang, S.-G., Clardy, J. and Scheraga, H.A. (1984) *J. Am. Chem. Soc.*, **101**, 7946–7958.

Montelione, G.T., Lyons, B.A., Emerson, S.D. and Tashiro, M. (1992) *J. Am. Chem. Soc.*, **114**, 10974–10975.

Piotto, M., Saudek, V. and Sklenář, V. (1992) *J. Biomol. NMR*, **2**, 661–665.

Ponder, J.W. and Richards, F.M. (1987) *J. Mol. Biol.*, **193**, 775–791.

Powers, R., Garrett, D., March, C., Frieden, E., Gronenborn, A. and Clore, G. (1993) *Biochemistry*, **32**, 6744–6762.

Redfield, A.G. and Waelder, S. (1979) *J. Am. Chem. Soc.*, **101**, 6151–6162.

Shaka, A.J., Keeler, J., Frenkiel, T. and Freeman, R. (1983) *J. Magn. Reson.*, **52**, 335–338.

Stonehouse, J., Shaw, G.L., Keeler, J. and Laue, E. (1994) *J. Magn. Reson.*, **A107**, 178–184.

Tolman, J.R. and Prestegard, J.H. (1996) *J. Magn. Reson.*, **B112**, 269–274.

Tycko, R., Pines, A. and Huckenheimer, R. (1985) *J. Chem. Phys.*, **83**, 2775–2802.

Wishart, D.S., Bigam, C.G., Holm, A., Hodges, R.S. and Sykes, B.D. (1995) *J. Biomol. NMR*, **5**, 67–81.

Wittekind, M. and Mueller, L. (1993) *J. Magn. Reson.*, **B101**, 201–205.

Wüthrich, K. (1986) *NMR of Proteins and Nucleic Acids*, Wiley, New York, NY, U.S.A.

Zhang, O., Kay, L.E., Olivier, J.P. and Forman-Kay, J.D. (1994) *J. Biomol. NMR*, **4**, 845–858.